

## Spin dynamics in the optical cycle of single nitrogen-vacancy centres in diamond

This content has been downloaded from IOPscience. Please scroll down to see the full text.

2011 New J. Phys. 13 025013

(<http://iopscience.iop.org/1367-2630/13/2/025013>)

View [the table of contents for this issue](#), or go to the [journal homepage](#) for more

Download details:

IP Address: 131.180.33.71

This content was downloaded on 16/03/2017 at 09:38

Please note that [terms and conditions apply](#).

You may also be interested in:

[Processing quantum information in diamond](#)

Jörg Wrachtrup and Fedor Jelezko

[Infrared emission of the NV centre in diamond](#)

L J Rogers, S Armstrong, M J Sellars et al.

[Nuclear spin induced collapse and revival shape of Rabi oscillations of a single electron spin in diamond](#)

Hu Xin, Liu Dong-Qi and Pan Xin-Yu

[Magnetic-field-dependent photodynamics of single NV defects in diamond: an application to qualitative all-optical magnetic imaging](#)

J-P Tetienne, L Rondin, P Spinicelli et al.

[Magnetometry with nitrogen-vacancy defects in diamond](#)

L Rondin, J-P Tetienne, T Hingant et al.

[Time-averaging within the excited state of the nitrogen-vacancy centre in diamond](#)

L J Rogers, R L McMurtrie, M J Sellars et al.

[Spin decoherence and relaxation processes in zero-dimensional semiconductor nanostructures](#)

M Chamarro, F Bernardot and C Testelin

[Excited-state spectroscopy of single NV defect in diamond using optically detected magnetic resonance](#)

P Neumann, R Kolesov, V Jacques et al.

## Spin dynamics in the optical cycle of single nitrogen-vacancy centres in diamond

Lucio Robledo<sup>1</sup>, Hannes Bernien, Toeno van der Sar  
and Ronald Hanson

Kavli Institute of Nanoscience Delft, Delft University of Technology,  
PO Box 5046, 2600 GA Delft, The Netherlands

E-mail: [l.m.robledo@tudelft.nl](mailto:l.m.robledo@tudelft.nl)

*New Journal of Physics* **13** (2011) 025013 (11pp)

Received 6 October 2010

Published 21 February 2011

Online at <http://www.njp.org/>

doi:10.1088/1367-2630/13/2/025013

**Abstract.** We investigate spin-dependent decay and intersystem crossing (ISC) in the optical cycle of single negatively charged nitrogen-vacancy (NV) centres in diamond. We use spin control and pulsed optical excitation to extract both the spin-resolved lifetimes of the excited states and the degree of optically induced spin polarization. By optically exciting the centre with a series of picosecond pulses, we determine the spin-flip probabilities per optical cycle, as well as the spin-dependent probability for ISC. This information, together with the independently measured decay rate of singlet population, provides a full description of spin dynamics in the optical cycle of NV centres. The temperature dependence of the singlet population decay rate provides information about the number of singlet states involved in the optical cycle.

### Contents

<b>1. Introduction</b>	<b>2</b>
<b>2. Experimental setting</b>	<b>2</b>
<b>3. Model</b>	<b>2</b>
<b>4. Spin-dependent lifetime</b>	<b>3</b>
<b>5. Temperature dependence of singlet decay</b>	<b>5</b>
<b>6. Polarization probability</b>	<b>7</b>
<b>7. Summary</b>	<b>10</b>
<b>Acknowledgments</b>	<b>10</b>
<b>References</b>	<b>10</b>

<sup>1</sup> Author to whom any correspondence should be addressed.

## 1. Introduction

Nitrogen-vacancy (NV) centres in diamond are well-defined quantum systems in the solid state, with excellent spin coherence properties [1]. Even in ambient conditions, NV centres have successfully been used in the fields of quantum information processing [2]–[8], magnetic sensing [9]–[13] and photonic devices [14]–[19]. However, despite rapid experimental progress, an understanding of the optically induced spin dynamics of the NV centre is still incomplete. In particular, the spin-dependent intersystem crossing (ISC) rates as well as the number of singlet states involved in the optical cycle are still debated. These parameters are responsible for optical spin initialization and readout, and are important for a correct estimation of photon emission rates. We extract these values by a series of room temperature experiments, where we perform spin-resolved fluorescence lifetime measurements using picosecond optical excitation pulses. The lifetime of the singlet manifold is measured by analysing the initial fluorescence rate for consecutive microsecond optical pulses with variable delay. The temperature dependence of this lifetime yields insights into the number of singlet states involved.

## 2. Experimental setting

We investigate individual NV centres contained in a high-temperature high-pressure (HTHP) grown-type IIa diamond sample from Element Six ( $\langle 111 \rangle$ -oriented). The sample is studied in a scanning confocal microscope setup operated at  $T = 10, \dots, 300$  K. Spin control is achieved via microwave (MW) fields applied to a gold waveguide that is lithographically defined on the diamond surface [6, 8]. For optical excitation, we use a continuous-wave (CW) laser at  $\lambda = 532$  nm, equipped with an acousto-optic modulator (AOM) with a 20 ns rise time, as well as a frequency-doubled diode laser at  $\lambda = 532$  nm with a pulse length of 62 ps (max. pulse energy: 25 nJ) and variable repetition rate. For photon detection, we use an avalanche photo-diode in the single-photon counting regime with a timing jitter of 450 ps. Time-resolved data are acquired using a time-correlated single-photon counting module with a jitter of 10 ps, using a bin size of 512 ps. An arbitrary waveform generator (channel-to-channel jitter  $< 100$  ps) is used as the timing source of the experiment.

## 3. Model

The photo-dynamics of the NV centre (figure 1(a)) are determined by six electrons, which in the ground state form a triplet occupying an orbital of  ${}^3A_2$  symmetry. The centre can be excited via a dipole-allowed transition to a  ${}^3E$  triplet state. This level also has a spin-dependent probability of undergoing ISC to a series of singlet states [20]. We use a five-level model to describe the spin dynamics of the NV centre (figure 1(b)). Spin–spin interaction splits the  ${}^3A_2$  ground state by  $D_{GS} = 2.87$  GHz into a state with spin projection  $m_s = 0$  ( $|1\rangle$ ) and a doublet with  $m_s = \pm 1$  (summarized in  $|2\rangle$ ). Correspondingly, the excited  ${}^3E$  state is labelled  $|3\rangle$  ( $m_s = 0$ , associated with a lifetime  $T_{1,|3\rangle}$ , where  $T_{1,|n\rangle}$  denotes the relaxation time of state  $|n\rangle$ ) and  $|4\rangle$  ( $m_s = \pm 1$ , lifetime  $T_{1,|4\rangle}$ ), and split by  $D_{ES} = 1.43$  GHz [21, 22].

Two singlet states with a splitting of  $\Delta E = 1.189$  eV have been identified experimentally [23, 24], but recent theoretical studies [25] and also data obtained in this work suggest the presence of a third singlet state between  ${}^3A_2$  and  ${}^3E$ . For the analysis of spin dynamics, however,

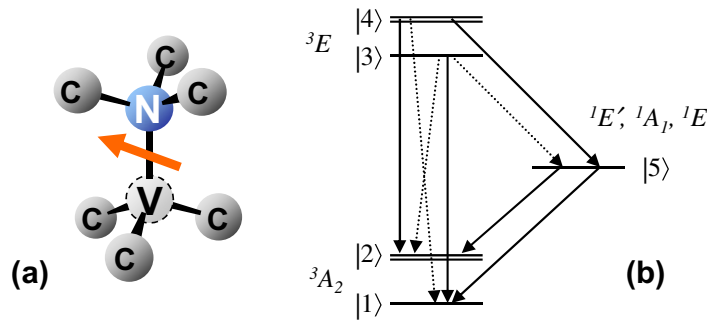


**Figure 1.** (a) Lattice structure of the NV centre: a substitutional nitrogen atom N next to a vacancy V in the diamond lattice C. (b) Level structure of the NV centre: we consider spin-conserving ( $k_{31}$ ,  $k_{42}$ ) and spin-flip ( $k_{32}$ ,  $k_{41}$ ) transitions between triplets (states with spin projection  $m_s = \pm 1$  are merged into states |2>, |4>). Spin-dependent ISC rates connect triplets to the singlet states (summarized as |5>) and described by rates  $k_{35}$ ,  $k_{45}$ ,  $k_{51}$ ,  $k_{52}$ ). As discussed in section 6, we assume  $k_{32}$ ,  $k_{41} \ll k_{31}$ ,  $k_{42}$  and find that  $k_{35} \ll k_{45}$ , but  $k_{51} \approx k_{52}$ .

we summarize the singlet states in |5>, and the corresponding lifetimes are summed and denoted as  $T_{1,|5\rangle}$ . Rates from state | $m$ > to state | $n$ > are denoted by  $k_{mn}$ , and we only consider relaxation rates indicated in figure 1(b). Population in state | $n$ > is denoted by  $P_n$ , and the spin polarizations in the ground and excited states are denoted by  $\mathbb{P}_{\text{GS}} = P_1/(P_1 + P_2)$  and  $\mathbb{P}_{\text{ES}} = P_3/(P_3 + P_4)$ .

#### 4. Spin-dependent lifetime

Pulsed optical excitation and time-resolved detection of fluorescence provide a simple and direct way to determine the lifetime of the excited state in an optical transition. If the excitation pulse is short compared to the lifetime  $T_1$ , the detected time-resolved fluorescence (averaged over many excitation cycles) decays exponentially  $I \propto \exp(-t/T_1)$ . However, if the system under consideration is excited into a mixture of  $n$  excited states with different lifetimes, the detected fluorescence decays according to a multi-exponential function  $I \propto \sum_n a_n \exp(-t/T_{1,|n\rangle})$ .

This situation is present in the case of NV centres in diamond, where the excited state is composed of a spin triplet. Population in this state decays radiatively to the triplet ground state, where we assume the different spin projections to have identical oscillator strength, based on the observation that the initial fluorescence rate is independent of the spin state as observed in [26] and as shown at a later point in this section. However, because of spin-dependent ISC [20], the effective lifetime of the excited state is significantly different for states |3> and |4>. In the literature [22, 26, 27], the NV centre's lifetime generally is obtained by fitting the time-resolved fluorescence to a single-exponential decay, leading to values of  $T_{1,|3\rangle} \approx 12\text{--}13$  ns and  $T_{1,|4\rangle} \approx 8$  ns in bulk diamond. Since optically induced spin polarization in NV centres is limited [28, 29], in fact we expect such a lifetime measurement to yield a bi-exponential decay curve with time constants set by the sums of rates out of states |3> and |4> [ $T_{1,|3\rangle} = 1/(k_{31} + k_{32} + k_{35})$  and  $T_{1,|4\rangle} = 1/(k_{41} + k_{42} + k_{45})$ ] and amplitudes  $a_n$  determined by the initial spin polarization. Such a bi-exponential decay has been observed in [29], where a polarization of  $\mathbb{P}_{\text{ES}} = 0.84 \pm 0.08\%$  has been obtained. These data are based on fluorescence

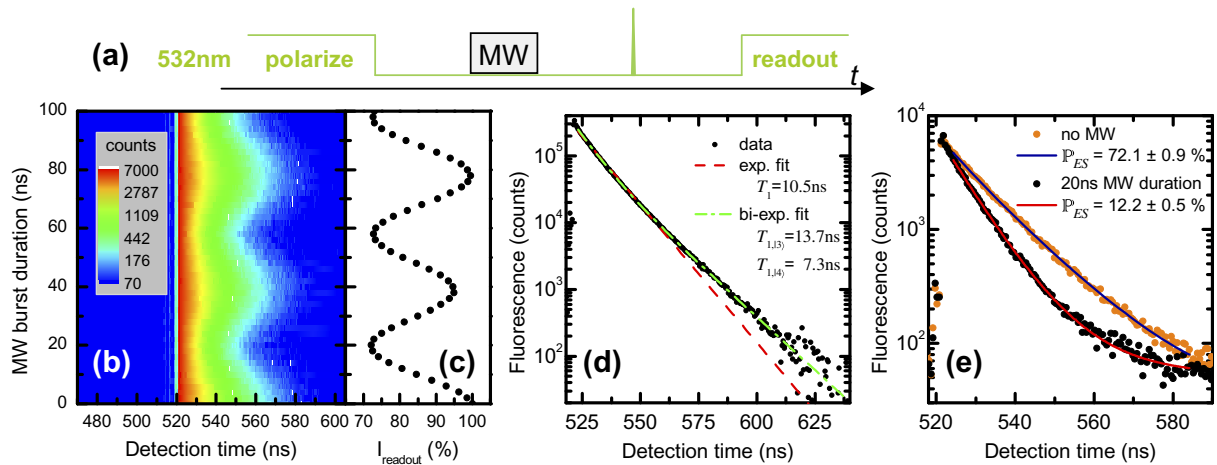


**Figure 2.** (a) We first polarize the spin by applying a  $1.3 \mu\text{s}$  laser pulse at  $\lambda = 532 \text{ nm}$ . After  $800 \text{ ns}$ , we turn on an MW field at  $2.87 \text{ GHz}$  for variable duration. At  $200 \text{ ns}$  after the beginning of the MW, we excite the NV centre by a  $62 \text{ ps}$  laser pulse at  $\lambda = 532 \text{ nm}$  and measure the time-resolved emission. The first  $300 \text{ ns}$  of the subsequent polarization pulse are used for spin readout. The experiment was performed at  $T = 300 \text{ K}$ . (b) Fluorescence decay as a function of MW burst duration (fluorescence counts are encoded in a logarithmic colour scale). The decay time oscillates with the  $m_s = 0$  amplitude, as confirmed by (c) conventional spin readout. (d) Fluorescence decay curve, integrated over all applied MW burst durations (a constant background has been subtracted). A fit using a bi-exponential function yields the lifetime of states  $|3\rangle$  and  $|4\rangle$ . A single-exponential function (shown for comparison) cannot accurately fit the experimental data. (e) Degree of spin polarization  $\mathbb{P}_{ES} = P_3/(P_3 + P_4)$  with no MW applied and after a  $20 \text{ ns}$  MW pulse, obtained from the relative amplitudes of a bi-exponential fit.

lifetime measurements with MW spin manipulation in the excited state, where the duration of the MW pulse was neglected, and the pulse was assumed to be perfect.

Here, we present a simple and reliable way to obtain the spin-dependent lifetimes, without any assumptions about the MW pulse and spin polarization. For that purpose, we drive Rabi oscillations in a conventional fashion, i.e. we apply a  $1.3 \mu\text{s}$  long off-resonant laser pulse to polarize the electron spin, followed by an MW pulse of variable duration, resonant with the zero-field splitting of  $D = 2.87 \text{ GHz}$ . After the MW, we apply a ps laser pulse. The fluorescence as a function of MW pulse duration is shown in figure 2(b). For comparison, we also plot the result of a conventional spin readout (figure 2(c)), i.e. the fluorescence integrated over the first  $300 \text{ ns}$  of the subsequent polarization laser pulse [30]. The data in figure 2(b) clearly reveal the oscillations in decay time, which are in phase with oscillations of the electron spin. We note that the maximum amplitude changes by less than  $1\%$  as a function of the spin state, consistent with our initial assumption about the oscillator strength. To accurately fit these data to a bi-exponential decay, we sum over all MW pulse durations, which gives similar contributions from each spin state. From the fit we obtain the two time constants  $T_{1,|3\rangle} = 13.7 \pm 0.1 \text{ ns}$  and  $T_{1,|4\rangle} = 7.3 \pm 0.1 \text{ ns}$  (figure 2(d)). By using these values as constants for a fit to the individual

decay curves, we can determine the relative contributions of states  $|3\rangle$  and  $|4\rangle$  to the minima and maxima of the Rabi oscillation data from the relative amplitudes of the two exponentials. For this particular centre, we find  $\mathbb{P}_{\text{ES,max}} = 72.1 \pm 0.9\%$  and  $\mathbb{P}_{\text{ES,min}} = 12.2 \pm 0.5\%$  (figure 2(e)). The value of  $\mathbb{P}_{\text{GS,max}}$  may be larger due to a non-perfect spin conservation in optical excitation (see section 6). For other centres, we find values for  $\mathbb{P}_{\text{ES,max}}$  of  $72.4 \pm 0.9$ ,  $79.4 \pm 0.2$  and  $81.7 \pm 0.9\%$ . The optically induced spin polarization may also depend on the probability of the NV centre occupying the neutral charge state  $\text{NV}^0$ . When switching from the neutral to the negative charge state under optical excitation, the spin state will likely be random, thus lowering the observed spin polarization of  $\text{NV}^-$ . Here, we took care to work with centres with an  $\text{NV}^0$  contribution of less than 5% to the overall emission.

The discrepancy between  $\mathbb{P}_{\text{ES,max}}$  and  $1 - \mathbb{P}_{\text{ES,min}}$  is a consequence of the  $S = 1$  nature of the NV ground state: for a spin  $S = 1$  system with degenerate levels  $m_s = \pm 1$  (i.e. for NV centres in the absence of magnetic field), the effect of resonant MW driving starting from a pure  $|m_s = 0\rangle$  state is to cause coherent oscillations between  $|m_s = 0\rangle$  and the symmetric superposition  $|m_s = +1\rangle + |m_s = -1\rangle$ . In a more realistic scenario, we need to consider an only partially polarized state, where the density matrix subspace spanned by  $|m_s = +1\rangle$  and  $|m_s = -1\rangle$  has equal population of the symmetric and antisymmetric superposition states. Only the symmetric state will be transferred back to  $|m_s = 0\rangle$ , so the effect of a half-oscillation is to transfer the full  $m_s = 0$  population into  $m_s = \pm 1$ , while only half of the incoherent population in  $m_s = -1$  and  $m_s = +1$  is transferred back into  $m_s = 0$ . As a consequence, when driving Rabi oscillations, the maximum population in  $m_s = 0$  will only reach half of the value of the maximum population in  $m_s = \pm 1$  (figure 2(e):  $\mathbb{P}_{\text{ES,min}} \approx (1 - \mathbb{P}_{\text{ES,max}})/2$ ).

In summary, the presented method allows for accurate determination of the lifetime of the pure states  $|3\rangle$  and  $|4\rangle$ , without the need for assumptions about the quality of spin manipulation. The knowledge of these lifetimes can then be used to quantify the spin polarization.

## 5. Temperature dependence of singlet decay

An important parameter for the spin dynamics of the NV centre under optical excitation is the time the population spends in the singlet manifold before it decays back to the triplet ground state. This time scale is long compared to the excited state lifetime, and since ISC into the singlet states occurs more likely out of the  $m_s = \pm 1$  than out of the  $m_s = 0$  excited state, this leads to a reduced fluorescence rate for  $m_s = \pm 1$ . This fact is routinely used for non-resonant spin readout [30].

The temperature dependence of this decay rate yields information about the energy splitting involved in this relaxation process, and adds further evidence for the number of singlet states contributing to the optical cycle of NV centres. Recently, an infrared (IR) emission channel was observed, and attributed to a dipole-allowed transition between two singlet levels with an energy splitting of  $\Delta E = 1.189$  eV [23, 24]. In the same publications, it was shown that the IR emission follows the same time dependence as the visible transition, implying a short lifetime of the upper singlet state. Therefore, the previously observed long-lived singlet state was attributed to the ground state of this IR transition.

The temperature dependence of this singlet state lifetime has been reported for an ensemble of NV centres based on IR absorption measurements [24]. Here, we present data obtained on single NV centres. Since the oscillator strength of the IR transition is very weak, we use an indirect way to obtain this timescale, following the method used in [20]: we first apply a green

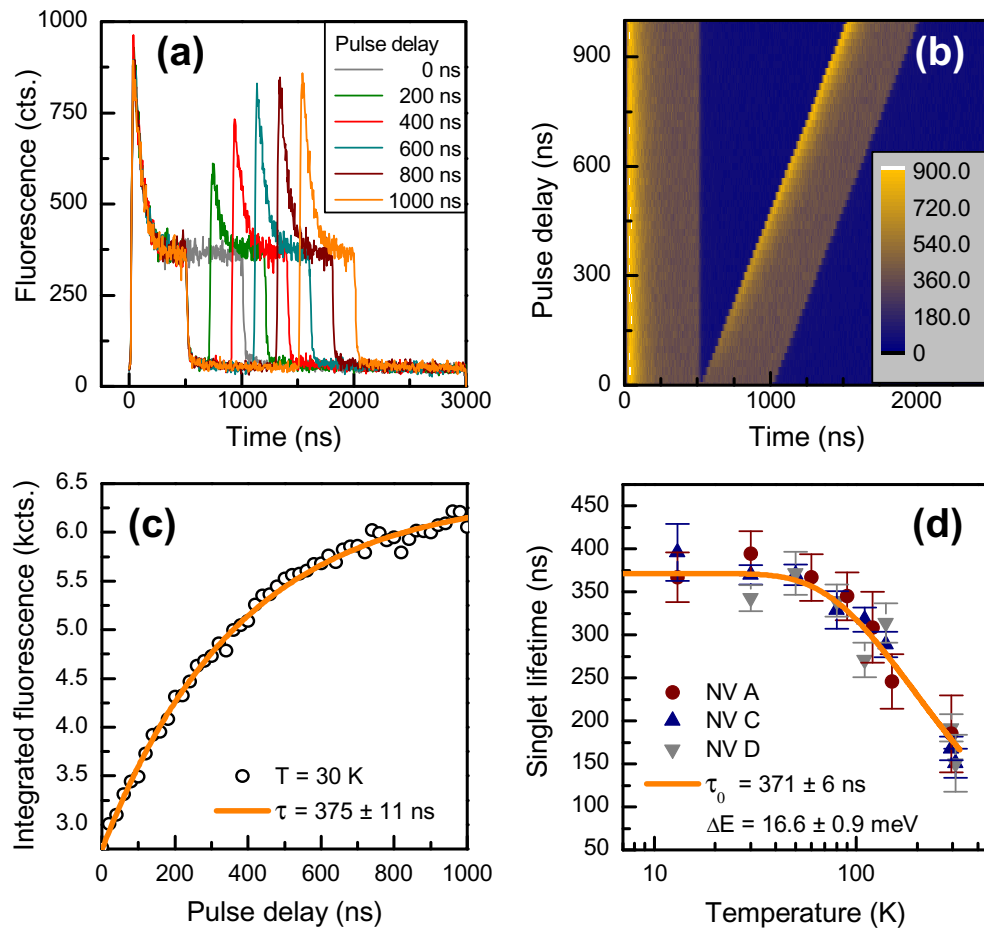


**Figure 3.** Decay of the population from singlet states leads to the recovery of fluorescence: (a) individual traces and (b) the full data set of NV fluorescence with two excitation pulses and variable delay. (c) Fluorescence counts integrated over the first 30 ns of the second pulse as a function of interpulse delay. The exponential increase is caused by decay out of singlet states. (d) Temperature dependence of singlet decay rate. The fit assumes a phonon-assisted decay process.

pulse (500 ns) to reach a significant population of the singlet states. This population manifests itself in reduced steady-state fluorescence with respect to the beginning of the pulse. After a variable delay, we apply a second 500 ns pulse (figures 3(a) and (b)). During the delay between the pulses, the population stored in the singlet states decays back to the triplet ground state. The fluorescence at the beginning of the second pulse is proportional to the population in the triplet ground state and thus we can attribute its dependence on interpulse delay to the population decay out of the singlet state. In figure 3(c), we integrate the photons emitted during the first 30 ns of the second pulse for each interpulse delay and fit these data to an exponential function. Figure 3(d) summarizes the timescales we obtained in this way, for temperatures ranging from  $T = 13$  K to  $T = 300$  K for three different NV centres.

We model the lifetime  $\tau$  of the singlet state as a combination of the temperature-independent spontaneous decay rate  $\tau_0^{-1}$  and a rate accounting for stimulated emission of phonons of energy  $\Delta E$  with an occupation given by Bose–Einstein statistics:  $\tau = \tau_0[1 - \exp(-\Delta E/k_B T)]$ . The fit yields a spontaneous emission lifetime of  $\tau_0 = 371 \pm 6$  ns and a phonon energy of  $\Delta E = 16.6 \pm 0.9$  meV, in reasonable agreement with ensemble data obtained in [24].

This result suggests that, apart from the 1.189 eV splitting, a third level  $\Delta E$  below the IR transition's ground state is involved in the optical cycle of the NV centre. We can exclude that this third level is the triplet ground state, just 16.6 meV below the lowest singlet, as this would imply phonon-assisted spin relaxation on a sub-microsecond timescale at room temperature. This scenario clearly contradicts experimentally observed spin lifetimes on a millisecond timescale [5, 8]. Consequently, the third level is likely to be another singlet state. The presence of three singlet states in between the triplet  $^3A_2$  and  $^3E$  states was recently predicted by an *ab-initio* calculation of the excited states in the NV centre [25]; however, there, a larger energy splitting between the lowest singlet states was obtained.

## 6. Polarization probability

Polarizing the electron spin by off-resonant optical excitation is a key technique for the room temperature spin manipulation of NV centres. Although this effect has already been identified to be caused by a spin-dependent ISC rate [20], [31]–[33], little is known about the relative contributions of spin-flip transitions between triplet states ( $k_{32}$ ,  $k_{41}$ ) and ISC rates ( $k_{35}$ ,  $k_{45}$ ,  $k_{51}$ ,  $k_{52}$ ). We address this question by determining the polarization change due to a single excitation cycle.

For that purpose, we first initialize the NV spin by a  $2 \mu\text{s}$  polarization pulse. After a waiting time of  $1 \mu\text{s}$ , we excite the NV centre by a reference ps pulse and measure the spin polarization by analysing the relative contributions of the amplitudes in a bi-exponential fit to the fluorescence decay curve, as outlined in the previous section. This polarization corresponds to the steady-state value after CW excitation. To determine the change in polarization per excitation cycle, we now apply an MW pulse to transfer the  $m_s = 0$  population into the  $m_s = \pm 1$  states and then drive individual excitation cycles by applying ten consecutive ps pulses separated by  $2 \mu\text{s}$ . For each excitation cycle, we again determine the spin polarization (figure 4(c)). All of these bi-exponential fits use the same two time constants, obtained from a fit to the sum of all decay curves. From a power dependence measurement of the NV fluorescence rate, we determine an excitation probability per ps pulse of  $\alpha = 0.95 \pm 0.05$ .

The effect of a single excitation cycle on the spin polarization can be described by two counter-acting probabilities: a spin-flip from  $|1\rangle$  to  $|2\rangle$  ( $p_{12}$ ) and the opposite process ( $p_{21}$ ). Here, we consider only optically induced effects, i.e. the time between excitation pulses  $\Delta_t$  is assumed to be much shorter than the spin-lattice relaxation time (this assumption is substantiated by the constant polarization  $P_{\text{ES}}$  for the ten consecutive reference pulses in the case of NV C (figure 4(c)). For state  $|m\rangle$ , the population just before pulse  $n$  is denoted by  $P_{m,n}$  and just after the excitation pulse by  $P'_{m,n}$ . The steady-state value  $P_{m,n=\infty}$  is abbreviated as  $P_m$ . The pulse separation  $\Delta_t$  is much larger than the singlet decay time, such that  $P_{1,n} + P_{2,n} = 1$  and therefore  $\mathbb{P}_{\text{GS},n} = P_{1,n}/(P_{1,n} + P_{2,n}) = P_{1,n}$ .

Experimentally, we obtain spin polarization in the excited state. This differs from the ground state polarization due to a fraction  $\epsilon = k_{23}/k_{13} = k_{14}/k_{24}$  of spin non-conserving



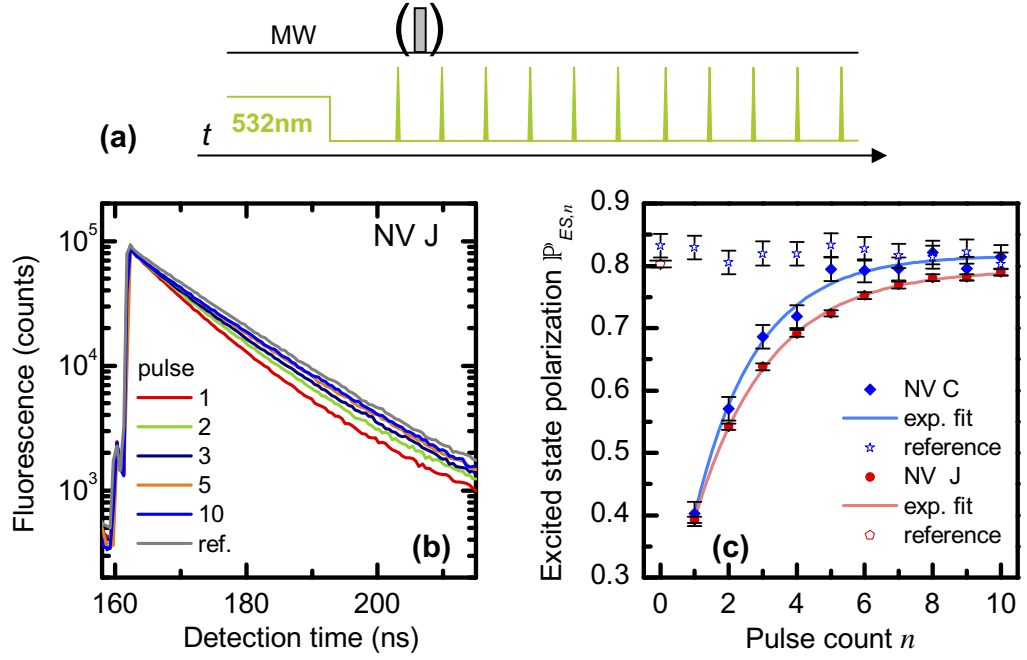


**Figure 4.** (a) We first polarize the spin by means of a  $2 \mu\text{s}$  laser pulse at  $\lambda = 532 \text{ nm}$ . After a delay of  $1 \mu\text{s}$ , we apply a sequence of 11 pulses of  $62 \text{ ps}$  duration at  $\lambda = 532 \text{ nm}$ . For NV J, we apply an MW pulse  $1 \mu\text{s}$  after the first ps pulse to invert the spin state (for NV C we alternately run sequences with and without MW pulse). For each ps-pulse, we measure the time-resolved emission. The experiment was performed at  $T = 300 \text{ K}$ . (b) Fluorescence decay for consecutive ps-excitation pulses. The decay follows a bi-exponential function. A reference ps pulse after a green  $2 \mu\text{s}$  spin polarization pulse yields the initial optically induced spin polarization. A subsequent MW pulse transfers polarization to  $|2\rangle$ . (c) Change in polarization between consecutive pulses yields spin-flip probabilities  $p_{12}(|1\rangle \rightarrow |2\rangle)$  and  $p_{21}(|2\rangle \rightarrow |1\rangle)$  per optical excitation cycle.

transitions. The populations for the  $(n + 1)$ th excitation pulse are then given by

$$P_{1,n+1} = \alpha p_{21} P_{2,n} + (1 - \alpha p_{12}) P_{1,n}, \quad (1)$$

$$P_{2,n+1} = \alpha p_{12} P_{1,n} + (1 - \alpha p_{21}) P_{2,n}, \quad (2)$$

$$P'_{3,n+1} = \alpha \left( \frac{\epsilon}{1 + \epsilon} P_{2,n+1} + \frac{1}{1 + \epsilon} P_{1,n+1} \right), \quad (3)$$

$$P'_{4,n+1} = \alpha \left( \frac{\epsilon}{1 + \epsilon} P_{1,n+1} + \frac{1}{1 + \epsilon} P_{2,n+1} \right). \quad (4)$$

The asymptotic value of the polarization is  $\mathbb{P}_{\text{GS}} = p_{21}/(p_{12} + p_{21})$ , and the excited state  $\mathbb{P}_{\text{ES},n} = P'_{3,n}/(P'_{3,n} + P'_{4,n}) = [P_{1,n}(1 - \epsilon) + \epsilon]/(1 + \epsilon) \approx P_{1,n}$  closely follows the ground state spin polarization for small  $\epsilon$ . In [20], an upper bound of  $\epsilon \leq 0.02$  is used, based on the maximum spin polarization of 80%. By comparison with a numerical solution of the rate equations of the five-level model outlined in section 2, we also find that the experimentally observed contrast

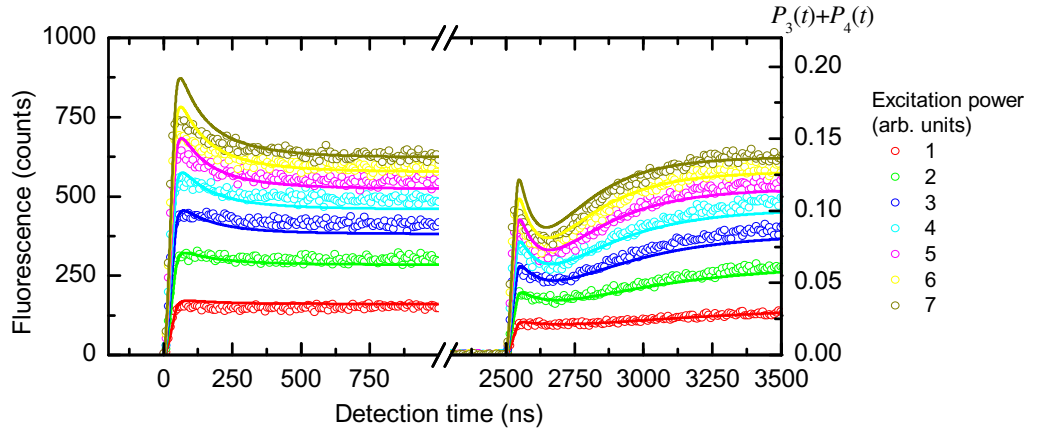


**Figure 5.** Time-resolved excitation-power dependence of NV fluorescence excited by off-resonant  $1 \mu\text{s}$  pulses (experimental data and model). The first pulse displays the fluorescence of NV centres that are optically polarized into  $m_s = 0$ . The second pulse is obtained after applying an MW  $\pi$ -pulse, representing the fluorescence of an NV centre polarized in  $m_s = \pm 1$ . The model shows the population in states  $|3\rangle$  and  $|4\rangle$ . The calculations are based on parameters from NV J, assuming  $\epsilon = 0.01$  and  $\alpha = 1$  (no fit is applied). Excitation rates are taken as integer multiples of 4 MHz.

**Table 1.** Summary of parameters ( $T = 300 \text{ K}$ ), taking  $\alpha = 0.95 \pm 0.05$  and  $\epsilon = 0.01 \pm 0.01$ . We used  $T_{1,|5\rangle} = 178 \pm 6 \text{ ns}$  from section 5.  $p_{12}$  and  $p_{21}$  are the total spin-flip probabilities per optical cycle.  $p_{35}$ ,  $p_{45}$ ,  $p_{51}$  and  $p_{52}$  are the spin-dependent ISC probabilities for population in states  $|3\rangle$ ,  $|4\rangle$  and  $|5\rangle$ .

	NV J	NV C
$p_{12}$	$0.078 \pm 0.002$	$0.079 \pm 0.004$
$p_{21}$	$0.315 \pm 0.011$	$0.372 \pm 0.017$
$T_{1, 3\rangle} (\text{ns})$	$13.26 \pm 0.03$	$13.1 \pm 0.1$
$T_{1, 4\rangle} (\text{ns})$	$6.89 \pm 0.06$	$7.0 \pm 0.2$
$p_{35}$	$0.14 \pm 0.02$	$0.17 \pm 0.03$
$p_{45}$	$0.55 \pm 0.01$	$0.56 \pm 0.02$
$p_{51}/p_{52}$	$1.15 \pm 0.05$	$1.6 \pm 0.4$

in spin readout (figure 5) is best reproduced by  $\epsilon \leq 0.02$ . The change in polarization per pulse (figure 4(c)) can be fitted by an exponential function  $\mathbb{P}_{\text{ES}}(n) = \mathbb{P}_{\text{ES}} + a \exp(-n/c)$ . From the steady-state polarization  $\mathbb{P}_{\text{ES}}$  and the polarization rate  $c$ , we can extract the spin-flip probabilities  $p_{21}$  and  $p_{12}$  per optical cycle. The values we obtain for  $p_{21}$  and  $p_{12}$  only weakly depend on  $\epsilon$  in the range  $\epsilon \leq 0.02$ . The results are summarized in table 1.

Based on the relations  $T_{1,|3\rangle} = 1/(k_{31} + k_{32} + k_{35})$ ,  $T_{1,|4\rangle} = 1/(k_{41} + k_{42} + k_{45})$  and  $T_{1,|5\rangle} = 1/(k_{51} + k_{52})$  (rates as indicated in figure 1(b)), we numerically solve the system of equations defining the five unknown rates  $k_{31}$ ,  $k_{35}$ ,  $k_{45}$ ,  $k_{51}$  and  $k_{52}$  using the measured parameters  $p_{12}$ ,  $p_{21}$ ,  $T_{1,|3\rangle}$ ,  $T_{1,|4\rangle}$ ,  $T_{1,|5\rangle}$  and assuming a fixed  $\epsilon = 0.01 \pm 0.01$ . In this way, we obtain the spin-dependent ISC probabilities  $p_{45} = k_{45}/(k_{41} + k_{42} + k_{45})$  and  $p_{35} = k_{35}/(k_{31} + k_{32} + k_{35})$ , and for the reverse process  $p_{51}/p_{52} = k_{51}/k_{52}$ . The results are summarized in table 1. The low values

of  $p_{51}/p_{52}$  are in contrast to the current picture of the singlet relaxation process, where  $p_{52} = 0$  was used [20]. This gives another hint that an additional  $^1E$  state needs to be considered for the relaxation process. The temperature dependence of  $p_{51}/p_{52}$  could give further insight into this topic.

We note that this set of parameters can be used to calculate the spin and power dependence of time-resolved NV centre emission using  $\mu\text{s}$  excitation pulses at  $\lambda = 532\text{ nm}$  within the framework of this five-level model. The numerical result qualitatively agrees with the experimental data (figure 5); however, for higher excitation rates, the model overestimates the initial fluorescence rate. This could be caused by a higher spin polarization of the centre from which we obtained experimental data in figure 5 compared to parameters of NV J, as used in the simulation.

## 7. Summary

We have experimentally determined the spin-dependent lifetime of the NV centre's excited state, whose difference is dominated by a spin-dependent ISC rate. Knowledge of these lifetimes allows us to determine the degree of spin polarization. In a second experiment, we identified the total lifetime of the singlet states and by analysing its temperature dependence, the energy splitting of the long-lived singlet transition. The measured energy of  $\approx 16\text{ meV}$  indicates that at least three singlet states are involved in the optical cycle of the NV centre. Finally, we determined the spin-dependent ISC probabilities by analysing the change of spin polarization induced by a single excitation cycle, without making assumptions about the number and nature of the singlet states. The results indicate that spin polarization is dominated by a preferential ISC out of the excited  $m_s = \pm 1$  states instead of a selective decay out of the singlets into the  $m_s = 0$  ground state. The obtained rates are consistent with spin-dependent NV fluorescence dynamics based on a five-level model.

## Acknowledgments

We thank V V Dobrovitski and L Childress for helpful discussions and Daniel Twitchen and Paul Balog of Element Six for provision of the diamond sample. This work was supported by the Foundation for Fundamental Research on Matter (FOM), the Netherlands Organisation for Scientific Research (NWO) and the EU programme SOLID. LR acknowledges support from the European Community under a Marie-Curie IEF fellowship.

## References

- [1] Balasubramanian G *et al* 2009 *Nat. Mater.* **8** 383
- [2] Jelezko F, Gaebel T, Popa I, Domhan M, Gruber A and Wrachtrup J 2004 *Phys. Rev. Lett.* **93** 130501
- [3] Childress L, Dutt M V G, Taylor J M, Zibrov A S, Jelezko F, Wrachtrup J, Hemmer P R and Lukin M D 2006 *Science* **310** 281
- [4] Dutt M V G, Childress L, Jiang L, Togan E, Maze J, Jelezko F, Zibrov A S, Hemmer P R and Lukin M D 2007 *Science* **316** 1312
- [5] Neumann P, Mizuochi N, Rempp F, Hemmer P, Watanabe H, Yamasaki S, Jacques V, Gaebel T, Jelezko F and Wrachtrup J 2008 *Science* **320** 1326
- [6] Fuchs G D, Dobrovitski V V, Toyli D M, Heremans F J and Awschalom D D 2009 *Science* **326** 1520

- [7] Neumann P, Beck J, Steiner M, Rempp F, Fedder H, Hemmer P R, Wrachtrup J and Jelezko F 2010 *Science* **329** 5991
- [8] de Lange G, Wang Z H, Ristè D, Dobrovitski V V and Hanson R 2010 *Science* **330** 60
- [9] Degen C 2008 *Appl. Phys. Lett.* **92** 243111
- [10] Taylor J M, Cappellaro P, Childress L, Jiang L, Budker D, Hemmer P R, Yacobi A, Walsworth R and Lukin M D 2008 *Nat. Phys.* **4** 810
- [11] Maze J R *et al* 2008 *Nature* **455** 644
- [12] Balasubramanian G *et al* 2008 *Nature* **455** 648
- [13] de Lange G, Ristè D, Dobrovitski V V and Hanson R 2010 arXiv:1008.4395
- [14] Fu K M C, Santori C, Barclay P E, Aharonovich I, Prawer S, Meyer N, Holm A M and Beausoleil R G 2008 *Appl. Phys. Lett.* **93** 234107
- [15] Babinec T M, Hausmann B J M, Khan M, Zhang Y A, Maze J R, Hemmer P R and Loncar M 2010 *Nat. Nanotechnol.* **5** 195
- [16] Hadden J P, Harrison J P, Stanley-Clarke A C, Marseglia L, Ho Y-L D, Patton B R, O'Brien J L and Rarity J G 2010 *Appl. Phys. Lett.* **97** 241901
- [17] van der Sar T, Hagemeyer J, Pfaff W, Heeres E C, Oosterkamp T H, Bouwmeester D and Hanson R 2010 arXiv:1008.4097
- [18] Siyushev P *et al* 2010 *Appl. Phys. Lett.* **97** 241902
- [19] Englund D *et al* 2010 *Nano Lett.* **10** 3922
- [20] Manson N B, Harrison J P and Sellars M J 2006 *Phys. Rev. B* **74** 104303
- [21] Fuchs G D, Dobrovitski V V, Hanson R, Batra A, Weis C D, Schenkel T and Awschalom D D 2008 *Phys. Rev. Lett.* **101** 117601
- [22] Neumann P *et al* 2009 *New J. Phys.* **11** 013017
- [23] Rogers L J, Armstrong S, Sellars M J and Manson N B 2008 *New J. Phys.* **10** 103024
- [24] Acosta V M, Jarmola A, Bauch E and Budker D 2010 *Phys. Rev. B* **82** 201202(R)
- [25] Ma Y, Rohlfing M and Gali A 2010 *Phys. Rev. B* **81** 041204
- [26] Batalov A, Zierl C, Gaebel T, Neumann P, Chan I Y, Balasubramanian G, Hemmer P R, Jelezko F and Wrachtrup J 2008 *Phys. Rev. Lett.* **100** 077401
- [27] Collins A T, Thomaz M F and Jorge M I B 1983 *J. Phys. C: Solid State Phys.* **16** 2177
- [28] Harrison J, Sellars M J and Manson N B 2006 *Diam. Relat. Mater.* **15** 586
- [29] Fuchs G D, Dobrovitski V V, Toyli D M, Heremans F J, Weis C D, Schenkel T and Awschalom D D 2010 *Nat. Phys.* **6** 688
- [30] Jelezko F and Wrachtrup J 2004 *J. Phys.: Condens. Matter.* **16** R1089
- [31] Nizovtsev A P, Kilin S Y, Jelezko F, Popa I, Gruber A and Wrachtrup J 2003 *Physica B* **340** 106
- [32] Harrison J, Sellars M J and Manson N B 2004 *J. Lumin.* **107** 245
- [33] Nizovtsev A P, Kilin S Y, Jelezko F, Gaebel T, Popa I, Gruber A and Wrachtrup J 2005 *Opt. Spectrosc.* **99** 233